

NPS ARCHIVE
1961
FRAWLEY, M.

INVESTIGATION OF STREAM FUNCTIONS
OBTAINED THROUGH SECOND-ORDER
GEOSTROPHIC APPROXIMATIONS

MILDRED J. FRAWLEY

LIBRARY
U.S. NAVAL POSTGRADUATE SCHOOL
MONTEREY, CALIFORNIA

INVESTIGATION OF STREAM FUNCTIONS
OBTAINED THROUGH
SECOND-ORDER GEOSTROPHIC APPROXIMATIONS

* * * * *

MILDRED J. FRAWLEY

INVESTIGATION OF STREAM FUNCTIONS
OBTAINED THROUGH
SECOND-ORDER GEOSTROPHIC APPROXIMATIONS

by

MILDRED J. FRAWLEY

//

Lieutenant, United States Navy

Submitted in partial fulfillment of
the requirements for the degree of

MASTER OF SCIENCE
IN
METEOROLOGY

United States Naval Postgraduate School
Monterey, California
1 9 6 1

PPS Archive

1961

Frawley, M.

INVESTIGATION OF STREAM FUNCTIONS
OBTAINED THROUGH
SECOND-ORDER GEOSTROPHIC APPROXIMATIONS

by

Mildred J. Frawley

This work is accepted as fulfilling
the thesis requirements for the degree of

MASTER OF SCIENCE

IN

METEOROLOGY

from the

United States Naval Postgraduate School

ABSTRACT

By using the geostrophic approximation in various of the horizontal acceleration terms in the Eulerian equations for horizontal flow, wind components are computed from which relative vorticity is determined. The problem of obtaining a stream function is then reduced to solving a Poisson-type equation, thus avoiding the use of the balance equation.

Two different computation schemes for the x, y components of the 500-mb wind are investigated. The stream functions obtained from these methods are then compared with those obtained through the solution of the balance equation. The results of forecasts for 24 and 48 hours using the various stream functions with the barotropic model are also presented.

The writer wishes to express her appreciation to Professor George J. Haltiner of the U. S. Naval Postgraduate School for his assistance and guidance in this investigation.

Appreciation is also expressed to the personnel of the U. S. Navy Fleet Numerical Weather Facility for their cooperation during the preparation of this paper. The writer is especially indebted to Mr. Geirmundur 'Arnason for his many informative discussions and suggestions, and to Mr. Milton H. Reese for his assistance in programming.

TABLE OF CONTENTS

Section	Title	Page
1.	Introduction	1
2.	Background	3
3.	Procedures	6
4.	Results of Stream-Function Computations	13
5.	Results of Stream-Barotropic Prognoses	15
6.	Conclusions	18
7.	Bibliography	20
8.	Appendix I	21
 Table		
I.		9
II.		9
III.		12
IV.		17

Table of Symbols

f - the Coriolis parameter, $2 \Omega \sin \phi$, where ϕ is the geographical latitude.

\bar{f} - the mean value of the Coriolis parameter, $2 \Omega \sin 45^\circ$.

Z - the height of an isobaric surface.

g - the upward component of the apparent gravitational acceleration.

Φ - the geopotential. $\Phi = gZ$.

ζ - the relative vorticity. $\zeta = \frac{\partial v}{\partial x} - \frac{\partial u}{\partial y}$.

η - the absolute vorticity. $\eta = \zeta + f$.

ψ - the stream function for the non-divergent component of velocity.

∇^2 - horizontal Laplacian operator on a constant pressure surface.

$\bar{J}(A, B)$ - horizontal Jacobian operator, $\bar{J}(A, B) = \frac{\partial A}{\partial x} \frac{\partial B}{\partial y} - \frac{\partial A}{\partial y} \frac{\partial B}{\partial x}$.

1. Introduction.

It has been found that the use of the geostrophic approximation in the quasi-geostrophic barotropic model for numerical prediction gives rise to spurious anticyclogenesis [1]. It has further been shown that such errors can be eliminated by replacing geostrophic wind and geostrophic vorticity by wind and vorticity derived from a stream function, thus retaining only the divergence-free part of the wind.

The present method used by both the Joint Numerical Weather Prediction Unit (JNWPU) in Suitland, Md., and the U. S. Navy Fleet Numerical Weather Facility (FNWF), Monterey, Calif., to obtain a stream function is through the solution of the balance equation

$$\nabla^2 \psi + \nabla \psi \cdot \nabla f - \frac{2}{f} \left[\left(\frac{\partial^2 \psi}{\partial x \partial y} \right)^2 - \frac{\partial^2 \psi}{\partial x^2} \frac{\partial^2 \psi}{\partial y^2} \right] = \frac{\nabla^2 \Phi}{f} \quad (1)$$

where Φ is the geopotential. This equation, a non-linear partial differential equation of the Monge-Ampere type, may be elliptic in one part of the map, parabolic in another and hyperbolic in a third area. The problems encountered in obtaining significant solutions to this equation have been discussed by Arnason [2].

The purpose of this research is to examine the possibility of obtaining a stream function in a somewhat simpler manner. By using the geostrophic approximation in various of the horizontal acceleration terms in the Eulerian equations for horizontal flow, wind components may be computed from which the relative vorticity may be determined. The problem of obtaining the stream function is then reduced to solving the equation

$$\zeta = \nabla^2 \psi, \quad (2)$$

a Poisson-type equation readily solved by numerical methods. Thus the use of the balance equation may be avoided.

2. Background.

Assuming the hydrostatic approximation, and using pressure (p) as the vertical coordinate, the equation of motion may be expressed as

$$\frac{d\vec{V}}{dt} = -g \nabla_p Z - f \mathbf{k} \times \vec{V} . \quad (3)$$

In scalar component form, equation (3) becomes, upon expanding the acceleration components,

$$\begin{aligned} \frac{\partial u}{\partial t} + u \frac{\partial u}{\partial x} + v \frac{\partial u}{\partial y} + \omega \frac{\partial u}{\partial p} &= -g \frac{\partial z}{\partial x} + f v \\ \frac{\partial v}{\partial t} + u \frac{\partial v}{\partial x} + v \frac{\partial v}{\partial y} + \omega \frac{\partial v}{\partial p} &= -g \frac{\partial z}{\partial y} - f u \end{aligned} \quad (4)$$

where $\omega = \frac{dp}{dt}$.

Various approximations have been used to represent the actual wind. The simplest is the geostrophic approximation in which the entire acceleration is assumed to be identically zero, yielding

$$\vec{V}_g = -g f^{-1} \nabla_p Z \times \mathbf{k} . \quad (5)$$

A second approximation widely used is that the flow is gradient. With this assumption, tangential accelerations are omitted, but centripetal accelerations are retained.

The wind law to be used herein primarily consists of omitting the local time derivatives. In addition, since the results are to be applied to one level only in the present study, the acceleration terms involving the vertical velocity advection will be omitted. Thus equations (4)

reduce to

$$\begin{aligned} u \frac{\partial u}{\partial x} + v \frac{\partial u}{\partial y} &= -f v_g + f v \\ u \frac{\partial v}{\partial x} + v \frac{\partial v}{\partial y} &= +f u_g - f u \end{aligned} . \quad (6)$$

By introducing geostrophic wind components in various terms on the left-hand side of equation (6) the u , v components of the wind and the relative vorticity were obtained.

Once the relative vorticity had been computed, a stream function, Ψ , was obtained by solving the Poisson-type equation

$$\oint = \frac{g}{f} \nabla^2 \Psi \quad (7)$$

using the relaxation technique. The introduction of the coefficient $\frac{g}{f}$ is necessary to give the computed Ψ -field units of height. This Ψ -field as computed was then used to make 24- and 48-hour barotropic prognoses which were compared to forecasts of both the JNWPU and FNWF stream functions using the same barotropic model.

All computations were done on the Control Data Corporation Model 1604 Computer using the U. S. Navy Fleet Numerical Weather Facility's octagonal grid. This grid, centered on the pole and extending to approximately 10° N latitude, consists of 1977 grid points with a grid size of 381 km at 60° latitude. Geostrophic winds and geostrophic vorticity were also computed in order that the effects of the approximations introduced could be compared. Since it is known that the geostrophic approximation is poor in low latitudes, and that small errors in the pressure field will give relatively large errors in computed winds in this area, the sine of the latitude was not allowed to become smaller than $\sin 15^\circ$ throughout the computations.

Initial data used were the 500-mb heights for OOZ, 3 January 1958. The Ψ -fields for OOZ, 4 and 5 January 1958 were also computed in order

to compare the forecast fields with the computed.

3. Procedures.

Basically, two computation schemes were investigated to obtain approximations of the x, y components of the 500-mb wind. In the first method, geostrophic wind components were substituted in the partial derivatives of equations (6). Thus the following simultaneous system of equations is obtained:

$$\begin{aligned} \left(1 + \frac{1}{f} \frac{\partial v_g}{\partial x}\right) u + \left(\frac{1}{f} \frac{\partial v_g}{\partial y}\right) v &= u_g \\ \left(-\frac{1}{f} \frac{\partial u_g}{\partial x}\right) u + \left(1 - \frac{1}{f} \frac{\partial u_g}{\partial y}\right) v &= v_g \end{aligned} \quad (8)$$

These equations were then solved for u and v, with the following restrictions imposed:

(a) an arbitrary lower limit of .25 was imposed on the terms $\left(1 + \frac{1}{f} \frac{\partial v_g}{\partial x}\right)$ and $\left(1 - \frac{1}{f} \frac{\partial u_g}{\partial y}\right)$, in order to avoid conditions approaching inertial instability;

and (b) the determinant of the coefficients was not allowed to become smaller than .125, to avoid excessive wind speeds. The above method will hereinafter be designated as Method I.

The second method investigated, to be referred to as Method II, consisted of replacing all the velocity components in the horizontal acceleration terms of equations (6) by the geostrophic components. Equations (6) then become

$$\begin{aligned} u' &= u_g - \frac{u_g}{f} \frac{\partial v_g}{\partial x} - \frac{v_g}{f} \frac{\partial v_g}{\partial y} \\ v' &= v_g + \frac{u_g}{f} \frac{\partial u_g}{\partial x} + \frac{v_g}{f} \frac{\partial u_g}{\partial y} \end{aligned} \quad (9)$$

This method, though presumably a cruder approximation to the actual

wind, has the decided advantage of avoiding the arbitrary restrictions imposed in Method I, as well as a greater simplicity in programming.

Since the stream field obtained by Method II was very nearly the same as that obtained by Method I, one can consider the sequence of approximations obtained by the equations

$$\begin{aligned} u^{(n)} &= u_g - \frac{u^{(n-1)}}{f} \frac{\partial v^{(n-1)}}{\partial x} - \frac{v^{(n-1)}}{f} \frac{\partial v^{(n-1)}}{\partial y} \\ v^{(n)} &= v_g + \frac{u^{(n-1)}}{f} \frac{\partial u^{(n-1)}}{\partial x} + \frac{v^{(n-1)}}{f} \frac{\partial u^{(n-1)}}{\partial y} \end{aligned} \quad (10)$$

with $n = 1 \dots \dots \infty$. Method III consisted of computing $u^{(2)}$ and $v^{(2)}$.

After computing the wind fields for the various methods, and the geostrophic wind, $\bar{V}_g = -g f^{-1} \nabla_p z \times K$, for OOZ, 3 January 1958, the difference between computed and geostrophic wind speeds, $|\bar{V}| - |\bar{V}_g|$, was examined in order to assess the effects of the various approximations on the horizontal acceleration. In the regions of sharply defined cyclonic curvature, Method II produced the greatest decrease, and, in regions of anticyclonic curvature, the least increase in the geostrophic wind. This is to be expected as may be seen from gradient-wind considerations. When the geostrophic approximation is used in the acceleration terms, the latter will tend to be overestimated in regions of cyclonic curvature and thus reduce the wind too much below the geostrophic. Similarly, in the vicinity of a ridge, the geostrophic approximation in the acceleration will tend to underestimate the acceleration and thus the resulting increase of the wind over the geostrophic will be inadequate.

The introduction of the higher order approximation by Method III

tended to bring the wind speed again toward the geostrophic and, in regions of extreme cyclonic curvature, the computed speeds exceeded the geostrophic in some cases. This will be further discussed in connection with vorticity.

Tables 1 and 2 show representative values of the difference between computed and geostrophic wind speeds found in regions of strong curvature.

Table I: Maximum difference between computed and geostrophic wind speeds observed in selected areas of well-defined cyclonic curvature.

Location	Geostrophic wind speed	<u>Maximum reduction in geostrophic wind speed</u>		
		Method I	Method II	Method III
Eastern United States	50 to 58 mps	-17 mps	-26 mps	-8 mps
Eastern Atlantic	30 to 38 mps	-12 mps	-19 mps	-5 mps
Eastern Europe	30 to 38 mps	- 8 mps	-11 mps	-4 mps
Off East Coast of Asia	50 to 62 mps	-20 mps	-31 mps	-9 mps
Central Pacific	50 to 60 mps	-19 mps	-28 mps	-7 mps

Table II: Maximum difference between computed and geostrophic wind speeds observed in selected areas of well-defined anti-cyclonic curvature

Location	Geostrophic wind speed	<u>Maximum increase in geostrophic wind speed</u>		
		Method I	Method II	Method III
Off East Coast of North America	15 to 20 mps	13 mps	7 mps	9 mps
Siberia	25 to 31 mps	8 mps	6 mps	7 mps
Central Pacific	30 to 39 mps	18 mps	11 mps	12 mps
Western Canada	4 to 14 mps	3 mps	2 mps	2 mps

Next the fields of geostrophic vorticity, $\zeta_g = \frac{g}{f} \nabla^2 Z$, and relative vorticity, $\zeta = \frac{\partial v}{\partial x} - \frac{\partial u}{\partial y}$, were computed. As was expected, the derived values of cyclonic vorticity associated with the migratory lows and troughs were smaller than the corresponding geostrophic quantities, with the reverse true in the case of anticyclonic vorticity. As shown in Table III, Method II produced the greatest decrease in cyclonic vorticity and the least increase in anticyclonic vorticity. With the introduction of the higher-order approximation, Method III, the values of both the positive and negative vorticity centers increased over those obtained from the first two methods. Again, in regions of strong cyclonic shear, the maximum values exceeded the geostrophic. Further iterations using the technique of Method III were made to determine if the introduction of still higher-order approximations would indicate convergence.

The vorticity fields computed from $u^{(3)}$ and $v^{(3)}$ did show some reduction in the cyclonic vorticity maxima, but the negative vorticity values kept increasing. With the next iteration, $u^{(4)}$ and $v^{(4)}$, the values obtained in regions of strong relative vorticity produced overflow in the fixed-point computations of this parameter, which had been scaled for a maximum value of $253 \times 10^{-6} \text{ sec}^{-1}$. This suggests, perhaps, that the sequence of computed winds was not converging toward realistic values, at least in one particular region, having given rise to excessive vorticity values.

After the relative vorticity fields were computed, the Poisson equation $\zeta = \frac{g}{f} \nabla^2 \psi$ was solved for the stream function ψ using the

relaxation technique. This technique as programmed by FNWF scans through the field of ψ laterally using the extrapolated Liebmann method of computing a new point value

$$\psi_{ij}^{n+1} = \psi_{ij}^n + R_{ij} \quad (11)$$

where R_{ij} is equal to $\frac{\lambda}{4} \left(\nabla^2 \psi_{ij} - \frac{\bar{f}}{g} \right)$ and $\frac{\lambda}{4}$ is the relaxation factor, in this case 0.35. The 500-mb height field was used as the initial approximation.

Table III

Position of associated low		ξ_3	Maximum value of center of cyclonic relative vorticity		
			Method I	Method II	Method III
39N	10E	67	52	47	60
58N	22E	80	68	63	70
38.5N	33E	80	63	58	73
78.5N	88E	38	34	34	36
54N	147E	73	61	57	65
56N	164W	59	51	50	51
84N	135W	51	51	50	52
55N	71W	84	75	71	74
46N	23W	100	71	59	92

4. Results of Stream-Function Computations.

A comparison of the computed stream-function fields with those obtained by the FNWF solution of the balance equation reveals that, in all instances, the gradient of ψ between the pole and the grid boundaries is slightly greater for the fields computed by the methods of this study than for those computed through the balance equation, the difference varying from 200 to 400 feet in the cases studied. Through the relationship $\vec{V}_\psi = -\nabla\psi \times \mathbf{K}$, it is obvious, then, that on the average the non-divergent part of the wind, computed by the methods described herein, slightly exceeds that obtained through the balance equation. Since, however, the difference in the gradient is almost uniform from the boundaries to the pole, the difference in wind speed at any point would be only of the order of centimeters per second.

Considering only the stream-function fields computed by the methods of this study, the gradient of ψ between pole and grid boundaries was least for Method II, corresponding to the lowest wind speeds.

A comparison of the computed stream functions with the FNWF stream functions and the height fields themselves reveals that the placement of the major systems is the same in all cases. However, an examination of the stream fields obtained by Method I reveals that the decrease in the amplitude of the troughs is slightly greater than that observed between the height and the FNWF stream-function fields. This decrease in amplitude of the major troughs is extremely pronounced in the ψ -fields computed by Method II, presumably due to the underestimation

of the wind by this method as previously mentioned.

With the introduction of the higher order approximation, Method III, this pronounced weakening of the troughs is not observed, the amplitude of the features being approximately the same as those of the FNWF Ψ -fields.

5. Results of Stream Barotropic Prognoses.

Using the stream functions obtained by the various methods, 24- and 48-hour prognoses were made using the barotropic forecasting equation

$$\nabla^2 \frac{\partial \psi}{\partial t} + \mathcal{J}(\psi, \eta) - \frac{\mu \eta}{\psi} \frac{\partial \psi}{\partial t} = 0 \quad (12)$$

where \mathcal{J} is the Jacobian operator [3]. The term $-\frac{\mu \eta}{\psi} \frac{\partial \psi}{\partial t}$ is added to the non-divergent barotropic model to stabilize the ultra-long atmospheric waves. In these computations μ was assigned the value of 4, in accordance with the results of Cressman [4].

In order to have some basis for comparison, 24- and 48-hour prognoses were also made using the same model with the stream functions obtained through both the FNWF and the JNWPU solutions of the balance equation. For verification purposes, difference fields were formed and the "pillow" and root-mean-square error computed over the entire grid using the formulae

$$\text{Pillow} = \frac{\sum_{n=1}^{1977} (A-B)_n}{1977} \quad (13)$$

$$\text{RMSE} = \sqrt{\frac{\sum_{n=1}^{1977} [(A-B) - \text{Pillow}]_n^2}{1977}} \quad (14)$$

where A is the computed stream function value and B is the forecast value.

As can be seen from Table IV, no significant difference in either the "pillow" or root-mean-square error is apparent for the case studied.

However, it may be noted that the root-mean-square error for both the 24- and 48-hour forecasts is least for Method II and largest for Method III.

An examination of the error fields themselves showed a marked similarity in the regions of errors greater than 200 feet. The only major differences that could be noted were in an area north of the Hawaiian Islands, where Method III had a much larger error than other methods, and in an area south of Greenland, where both Methods I and II produced errors approximately 200 feet less than the other methods.

Since the barotropic model used for forecasting does not include provisions for development, only the movement of the major systems was used to compare the various methods. Considering only this aspect, no great differences appeared with regard to most of the major systems. The only notable exceptions were the troughs in the Eastern Pacific and the Eastern Atlantic where movement was overestimated less using the FNWF stream function than by the other methods. In addition, there was a slight indication that, at least in this case, the systems tended to move slightly faster when Method I was used.

Table IV

Method used to obtain initial stream function	24-hour baro- tropic forecast		48-hour baro- tropic forecast	
	Pillow	RMSE	Pillow	RMSE
FNWF solution of				
balance equation	+ 8 ft.	174 ft.	+ 6 ft.	272 ft.
JNWPU solution of				
balance equation	-36 ft.	172 ft.	-70 ft.	273 ft.
Method I	-14 ft.	169 ft.	-56 ft.	282 ft.
Method II	+9 ft.	164 ft.	+24 ft.	254 ft.
Method III	-17 ft.	182 ft.	-62 ft.	311 ft.

6. Conclusions.

Since the methods described herein have been applied to only one synoptic situation in this study, only tentative conclusions can be made at this point as to the relative merits of the various ways of obtaining a stream function for use in numerical prognostic models. All methods have shown comparable results and, until many different weather patterns are tested, it is difficult to separate the errors in the forecasts into those arising from inadequacies in the barotropic model and those due to the assumptions made in the various methods.

It has been seen, however, that the stream-function fields obtained from Method II had the least computed root-mean-square error of any of the methods tried and a "pillow" smaller than those computed using the other two methods of this study or the JNWPU solution to the balance equation for both the 24- and the 48-hour prognoses. However, a greater decrease in amplitude in the transition from the height to the stream-function field has also been observed when this method was used and must also be considered in evaluating this method. Although this method presumably underestimates the total wind speed, in the case studied the 24-hour prognostic movement of the major systems did not differ appreciably from that of the other methods used. Since no arbitrary restrictions need be imposed when this method is used, and since it is easier to program, further study is certainly warranted.

Since the introduction of the higher-order approximation into the same basic computation scheme (Method III) produced spurious results

in both the wind and the relative vorticity fields, the use of this procedure appears questionable. However, the introduction of certain restrictions on the values of $\frac{\partial v^{(n)}}{\partial x}$ and $\frac{\partial u^{(n)}}{\partial y}$, similar to those imposed in Method I, may possibly eliminate the difficulties encountered.

The procedure described under Method I apparently has some merits, although further study should be made of the arbitrary restrictions placed on this method for the computations of this study. It would also be most interesting to try further iterations of this method using equations of the form

$$\begin{aligned} \left(1 + \frac{1}{f} \frac{\partial v^{n-1}}{\partial x}\right) u^n + \left(\frac{1}{f} \frac{\partial v^{n-1}}{\partial y}\right) v^n &= u_g \\ \left(-\frac{1}{f} \frac{\partial u^{n-1}}{\partial x}\right) u^n + \left(1 - \frac{1}{f} \frac{\partial u^{n-1}}{\partial y}\right) v^n &= v_g \end{aligned} \quad (15)$$

to determine what the effect on the geostrophic deviation and relative vorticity would be in comparison to the effects observed upon introduction of the higher approximations in Method III. Since extensive reprogramming would be involved in doing this, such iterations were not attempted in this study.

Bibliography

1. Shuman, F. G., Prediction Consequences of Certain Physical Inconsistencies in the Geostrophic Barotropic Model, Monthly Weather Review, 85 (7), pp 229-234, July, 1957.
2. Arnason, G., A Convergent Method for Solving the Balance Equation, J. of Meteor., 15 (2), pp 220-225, April, 1958.
3. Haltiner, G. J., Weather Prognosis by Dynamical Methods, U. S. Naval Postgraduate School, Department of Meteorology, pp 1-27.
4. Cressman, G. P., Barotropic Divergence and Very Long Atmospheric Waves, Monthly Weather Review 86 (8), pp 293-297, August, 1958.

Appendix I

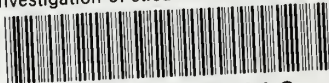
The following charts were computed during the course of this investigation and are available upon request from the U. S. Naval Postgraduate School, Monterey, California.

- (1) 500-mb heights, OOZ, 3 Jan. 1958
- (2) 500-mb heights, OOZ, 4 Jan. 1958
- (3) 500-mb heights, OOZ, 5 Jan. 1958
- (4) Geostrophic Wind Speed, OOZ, 3 Jan. 1958
- (5) Method I, 500-mb Wind Speed, OOZ, 3 Jan. 1958
- (6) Method II, 500-mb Wind Speed, OOZ, 3 Jan. 1958
- (7) Method III, 500-mb Wind Speed, OOZ, 3 Jan. 1958
- (8) Geostrophic Relative Vorticity, OOZ, 3 Jan. 1958
- (9) Method I, Relative Vorticity, OOZ, 3 Jan. 1958
- (10) Method II, Relative Vorticity, OOZ, 3 Jan. 1958
- (11) Method III, Relative Vorticity, OOZ, 3 Jan. 1958
- (12) FNWF Stream Function, OOZ, 3 Jan. 1958
- (13) Method I, Stream Function, OOZ, 3 Jan. 1958
- (14) Method II, Stream Function, OOZ, 3 Jan. 1958
- (15) Method III, Stream Function, OOZ, 3 Jan. 1958
- (16) FNWF Stream Function, OOZ, 4 Jan. 1958
- (17) Method I, Stream Function, OOZ, 4 Jan. 1958
- (18) Method II, Stream Function, OOZ, 4 Jan. 1958
- (19) Method III, Stream Function, OOZ, 4 Jan. 1958
- (20) FNWF Stream Function, OOZ, 5 Jan. 1958

- (21) Method I, Stream Function, OOZ, 5 Jan. 1958
- (22) Method II, Stream Function, OOZ, 5 Jan. 1958
- (23) Method III, Stream Function, OOZ, 5 Jan. 1958
- (24) FNWF 24-hr. Stream-Function Prognosis, Verifying Time, OOZ, 4 Jan. 1958
- (25) Method I, 24-hr. Stream-Function Prognosis, Verifying Time, OOZ, 4 Jan. 1958
- (26) Method II, 24-hr. Stream-Function Prognosis, Verifying Time, OOZ, 4 Jan. 1958
- (27) Method III, 24-hr. Stream-Function Prognosis, Verifying Time, OOZ, 4 Jan. 1958
- (28) Difference between FNWF Computed Ψ -field and Prognosis, OOZ, 4 Jan. 1958.
- (29) Difference between JNWPU Computed Ψ -field and Prognosis, OOZ, 4 Jan. 1958
- (30) Difference between Method I Computed Ψ -field and Prognosis, OOZ, 4 Jan. 1958
- (31) Difference between Method II Computed Ψ -field and Prognosis, OOZ, 4 Jan. 1958
- (32) Difference between Method III Computed Ψ -field and Prognosis, OOZ, 4 Jan. 1958

thesF786

Investigation of stream functions obtain



3 2768 001 95994 3

DUDLEY KNOX LIBRARY